DII-2

A LIMIT APPROACH TO THE PREVENTION OF PRESSURE VESSEL FAILURE

R. W. Nichols,[1] W. H. Irvine,[2]
A. Quirk[2] and E. Bevitt[2]

Abstract

The conditions giving rise to fast fracture initiation and propagation are discussed in relation to the case of a pressure vessel containing compressible fluid, with particular reference to the size of defect leading to ultimate failure. Experimental work carried out to provide numerical data is summarised and interpreted. The significance of the results is then considered in relation to the proposed use of higher design stresses, of new materials, and of particular environments, and with respect to the operational safety of nuclear reactor pressure circuits.

Introduction

Great practical advantages can, in some circumstances, arise if it is possible to state that the failure of a particular structure is absolutely beyond the realms of feasibility. Such a requirement leads to a limit approach to the problem of avoidance of failure. It is considered that such an approach can help more generally in the understanding of the conditions which could lead to eventual failure and thus help in providing economies in material by eventually allowing the possibility of higher design stresses.

It is a feature of most of the fracture mechanics approaches to such a problem that they indicate a tolerable defect size which will not propagate catastrophically at a specified stress level. Unfortunately it is not possible, even with the best of modern techniques for the production and inspection of components, to state with absolute certainty that a particular fabrication is free from flaws bigger than a certain size. This arises not only because of the limitations of inspection techniques, but also because of the possibility of human error. A technique which overcomes this limitation is that of proof stressing the finished structure before it is put into service, thus transferring the potential risk of failure to a time when one can be specially prepared. An example of this is the proof pressure test generally applied to pressure vessels, and it is suggested that, if such a test is done in a controlled way, it can be used to demonstrate absolutely that no flaws above a certain size can exist in the vessel at this stage in its life.

---

(1) U.K.A.E.A. Reactor Materials Laboratory, Culcheth, Warrington, Lancs.
(2) U.K.A.E.A. Health & Safety Branch (Safeguards Division), Risley, Warrington, Lancs.

Once such a vessel goes into service, however, factors such as changing stress and temperature conditions and various aspects of the service environment could lead to the growth of any sub-size flaws to a size where they would be capable of unstable propagation. Continued demonstration of freedom from the possibility of failure could result from further proof pressure tests at intervals throughout the life of a structure dictated by knowledge of the rate and mechanisms of the growths of cracks under various service conditions, and the numerical values of the parameters controlling crack instability.

During the last three years, work to this end has been proceeding in the U.K.A.E.A. This report is a description of the theoretical ideas and a summary of the experimental data to date. The results from both the experimental and theoretical work are applied to the study of operational safety, levels of design stress, radiation damage, and new high-strength materials.

Theoretical Considerations

The limit approach suggested in the introduction postulates that the necessary conditions for crack initiation and/or crack growth can arise in a pressure vessel and directs safety appraisal towards the conditions necessary for fast propagation of an unstable crack. Whilst undoubtedly the possibility of crack extension is determined primarily by the local stresses and strains in relation to the material properties at the crack tip, in a real structure these local stresses are related to the general applied load. The size of the plastic zone at the tip of a crack is a function both of the crack length and of the ratio of applied load to load needed to cause general yield.(1) It would thus appear to be reasonable to approach the problem via the relationship of gross stress to crack length, in the manner described by Irvine et al.(2).

Effect of Structure on Crack Propagation

It is first necessary to consider the effect of crack extension itself on the applied load and hence the level of gross stress. Two extreme situations can be considered, that of constant strain across the specimen, and that of constant stress. If the case of a crack in a flat sheet is considered, and if the system is one in which strain or deflection remains constant with crack extension, then no external work is done on the sheet and hence the decrease in strain energy equals the work available for dissipation in plastic deformation at the crack tip, the gross stress decreasing accordingly.

On the other hand, in an elastic system in which gross stress or load remains constant with crack extension, it can be shown that the work done by the load is divided equally between increasing the strain energy in the system and the energy available for dissipation in the crack tip region(3).

For both the constant stress and constant strain cases, at the point of instability the energy becoming available can be equated with that dissipated at the crack tip, leading to the Griffith-Orowan type of relationship:

$$f_g^2 l = \frac{EW}{2} \qquad \ldots\ (1)$$

where f_g = critical value of gross stress

l = half crack length

E = modulus of elasticity

W = material toughness or dissipation of energy in plastic deformation at crack tips for unit crack extension.

While equation (1) applies to both the constant strain and the constant stress cases and defines the onset of fast propagation, the sequence of events following this in the two cases may be vastly different. For instance, as a result of insufficient strain energy under constant strain conditions, the instability condition may often be masked by the consequent drop in stress and immediate arresting of the crack. Further straining results in this sequence being repeated, the crack propagating in a series of small jumps. Although, in the true constant-stress case, once the crack has become unstable an arrest cannot occur, there are cases in which the stress, although initially constant, undergoes a reduction due to extensive propagation of the crack, e.g. in a pressure vessel pressurised hydraulically, where propagation of the crack causes dilation of the vessel and finally leakage, with consequent loss of pressure and crack arrest.

In practice there may be deviations from these idealised conditions of strictly constant strain and constant stress; the difference between these two types of behaviour is nevertheless fundamental and usually well defined. This is an all-important aspect when the structure in which crack propagation tests are being carried out has different characteristics from the structure to which the tests are being applied. The case of a pressure vessel containing compressible fluid is close to the constant-stress case and therefore tests which are not carried out in an apparatus having similar unloading characteristics can lead to optimistic and unrealistic conclusions for this application.

Modes of Propagation

It has previously been postulated and demonstrated that three modes of fast propagation are possible for a cylindrical pressure vessel containing a longitudinal slit(2). Let P_1, P_2 and P_3 represent the principal stress system at the tip of the crack, where P_1 and P_2 act normal and parallel to the crack respectively and P_3 is the stress in the thickness direction. The constituent stresses of this stress system, and also for a flat plate, are outlined in Appendix I.

If the possible variation of these principal stresses through the material at a crack tip is considered for a flat plate under tension normal to the direction of the crack, and a pressure vessel under internal pressure respectively, we have:

(a) Plate

At the surface of the plate P_3 is zero and P_2 small and tensile in direction. Then assuming that P_1 is the maximum prinicpal stress, the maximum shear stress will be $P_1/2$.

However, at the plate mid-thickness, P_3 is at its maximum value, and consequently a tri-axial tensile stress system exists with low values of shear stress. Shear stress = $(P_1 - P_2)/2$ or $(P_1 - P_3)/2$ and P_2 and P_3 are large tensile stresses.

Consequently two types of failure can occur, those resulting from shear near the surfaces of the plate and those resulting from cleavage in the centre region of the plate thickness. However, the magnitude of P_1 is the controlling parameter in each case.

(b) Pressure Vessel

The conditions at the centre of the plate thickness in the region of a crack tip remain similar to plane plate conditions, i.e. a tensile triaxial stress system leading to cleavage type failure. However, the conditions at the outer surface have changed in that a tensile stress P_{2L} and compressive stress P_{2M} have been introduced (see Appendix I) where P_{2L} and P_{2M} are pressure and bending stresses respectively along the crack axis. The thickness stress P_3 is still zero at the surface so that large shear stresses exist in this region. However, if the compressive stress P_{2M} due to bulging of the unsupported length of the vessel is greater than the tensile components of P_2 then P_2 will become compressive near the outer surface and will have a maximum negative value on the outer surface, and the maximum shear stress will be $(P_1 - P_2)/2$, where P_2 is negative.

Thus there are three failure conditions for a crack in a vessel:

(i) Cleavage failure in mid-thickness, dependent on P_1

(ii) Shear failure at the outer surface.

For this case $P_3 = 0$ and P_2 is positive throughout the plate thickness so that the possibility of failure is dependent on $(P_1 - P_3)$. In general, this mode of failure will be characterised by a fracture running along the axis of the crack but inclined at 45° to the plate surface and will be referred to subsequently as $(P_1 - P_3)$ shear failure.

(iii) Shear failure at the outer surface dependent on $P_1 - P_2$, where P_2 is negative on the outer surface of the vessel. This mode of failure will be characterised by fractures originating at the crack tip and running at 45° to the axis of the crack and will be referred to subsequently as $(P_1 - P_2)$ shear failure.

Of these three failure modes, the first two are dependent only on the magnitude of P_1 whilst the last mode is dependent on $P_1 - P_2$. However, negative values of P_2 will be associated with appreciable bulging of the vessel in the neighbourhood of the crack, and will

occur only with cracks long in relation to the vessel diameter.

Assuming that crack extension occurs when the local stress exceeds a critical value, then the preceding paragraphs indicate that:

(i) Cleavage failure occurs if $P_1 = f_u$ .... (2a)

(ii) $(P_1 - P_2)$ shear failure occurs when $P_1/2 = f_s$ .... (2b)

(iii) $(P_1 - P_2)$ shear failure takes place when $(P_1 - P_2)/2 = f_s$ .... (2c)

where f_u and f_s are the ultimate failure stresses in tension and shear.

It will be noted that in a flat plate there are no effects which can cause P_2 to go negative, so the $P_1 - P_2$ shear mode cannot exist. Thus in comparing vessel and flat-plate tests the same failure curve would be followed for failures under cleavage P_1 and shear $(P_1 - P_3)$ modes. However, when $(P_1 - P_2)$ mode failures occur in a vessel, the flat plate would still be failing in accord with an extrapolation of the $(P_1 - P_3)$ mode, thus giving an optimistic failure criterion. It will be seen in the next section that another factor, the applied stress distribution, can have a much greater effect and give an optimistic failure criterion for all failure modes.

The Applied Stress Distribution in Flat-Plate Testing

Provided that a suitable testing machine is available, flat-plate testing has the advantage of economy and convenience compared with tests on actual vessels. However, it must be demonstrated that realistic fracture data are obtained from the tests.

It has already been shown that only two of the three modes of failure of a pressure vessel can occur in a flat plate. Nevertheless, it was thought worthwhile to carry out tests to study failure of defected flat plates in a machine at the U.K.A.E.A. Reactor Materials Laboratory originally designed to carry out wide-plate crack arrest tests. This machine is capable of applying a 4000 ton load to a specimen 4 ft long by 8 ft wide and 1 in. thick. However, the specimen is attached to essentially rigid cross beams by thick (compared to the test piece) attachments. The load is applied at the ends of the cross beams. The type of specimen is shown in Fig. 1 and the actual machine has been described by Winder(4). In this arrangement, when a specimen is tested, an essentially uniform deflection is applied across it. For example, if a load is applied to give a nominal stress of 10 tons/in^2 to a specimen with no test slit, then the specimen would increase in length by approximately 0.03 in.; because of the rigid nature of the loading attachments this deflection must remain constant across the width of the specimen. In this case, the applied stress will be uniformly distributed across the specimen, and an applied strain of 0.07% will be uniformly applied. If a specimen with a central through slit is now considered under similar loading

conditions, plastic zones several inches in diameter will exist at the slit extremities. The strain occurring in these plastic zones will account for a considerable amount of the total, and fixed, deflection which the rigid attachments are only able to apply in a uniform manner. The material above and below the plastic zones cannot therefore have as much deflection as that which occurred under similar conditions in the specimen with no crack. Thus the applied stress must be less in the centre of the top and bottom edges of the specimen with a slit than at similar positions in the specimen with no slit. Consequently, for a given mean stress, the stress applied to a slotted plate will be lower than the mean value at the centre, and higher at the edges. As a result, the P_1 stress at the tip of the slit will be less than if a uniformly distributed stress were applied to the specimen, and a higher mean value of stress will be required for fracture than would be required if a uniformly distributed stress was applied. Under extreme situations, part of the central area can be virtually unstressed, so that the specimen behaves as two specimens with edge notches of ill-defined depth. The effect becomes more pronounced the less the available deflection for a given load (i.e. the shorter the specimen between loading flanges) and the greater the size of the plastic zones (higher applied stresses and longer cracks). Thus, while it is possible for a particular apparatus to give meaningful results where failure occurs under brittle conditions with small plastic zones, it becomes increasingly difficult in considering specimens with increasing material toughness to get valid results from the rigid loading of a finite specimen.

Experimental assessment of these effects is described in a later section, and it is shown that data from such tests can be optimistically misleading.

The Relationship of Material Properties to the Fracture Constant

A possible approach to the general problem is to develop a system of fracture mechanics which will enable results obtained from the fracture of some standardised defected test pieces to be used to predict the behaviour of actual components. It is also desirable to relate the fracture constants used in such an approach to the conventional properties of the materials. The present state of knowledge does not permit such treatments by theoretical analysis alone. One difficulty is that we do not know the local criterion of failure. An associated and larger problem is that no general analytical solution yet exists for the magnitude of local stresses and strains in the vicinity of a crack except for the purely elastic case. It is thus necessary to see what relationships can be deduced from experimental results as a means of furthering this discussion.

The relationships of the general applied stress for crack extension to crack length has been examined in published work covering a wide range of materials and specimen geometries. This examination shows that the relationships governing the onset of instability takes the form:

$$f_g^3 l^2 = \text{constant} \qquad \ldots. (3)$$

The published literature covers 9 ft dia. x $\frac{3}{4}$ in. thick spherical steel pressure vessels tested at a Charpy value of 15 ft lb,(5) tests on flat sheets of various aluminium alloys of widths in the range 10 to 35 in.,(6-9) tests on aluminium alloy cylinders of 7.2 and 28.8 in. dia.,(10) tests on

5 ft dia. x 15 ft long steel cylindrical pressure vessels in both the brittle and ductile range(11) and tests on approximately 2 in. dia. zirconium tubes both irradiated and unirradiated(12). Even the early tests by Griffiths(13) on cylindrical glass tubes show a better fit to an f^3l^2 rather than an f^2l relation as shown in Table I(a) constructed from his original results.

It would appear that the parameter f^3l^2 has widespread applicability in governing fracture of a structure containing a defect, the value of this parameter representing a material property which is constant under particular environmental conditions (temperature, strain rate, chemistry) and over at least a limited range of structure geometries. Empirically it has been shown that a relationship of practical value exists, at least for a limited range of steels, between this constant and the Charpy V-notch energy value. We can now combine these two requirements to give failure relationships for the three types of failure described earlier. These are:

Cleavage failure: $$f_g^3 l^2 = f_y^d f_u^e (C + D\varphi) \qquad \ldots.(4a)$$

$(P_1 - P_3)$ shear failure: $$f_g^3 l^2 = f_y^d (2f_s)^e (C + D\varphi) \qquad \ldots.(4b)$$

$(P_1 - P_2)$ shear failure: $$f_g^3 l^2 = f_y^d (P_2 + 2f_s)^e (C + D\varphi) \qquad \ldots.(4c)$$

where φ represents the Charpy energy. The derivation of these equations is given by Irvine et al.(2) and they are based on the assumption that, because of the nature of the failure condition f^3l^2, it should be possible by dimensional analysis to relate the relevant parameters controlling P_1 in equation (2).

It will be noted that equation (4c) contains the stress P_2, the magnitude of which is dependent on the amount of bulging over the crack length. Consequently P_2 will be dependent on crack length, internal pressure and vessel thickness and diameter. It follows therefore that, in a particular vessel, an individual $(P_1 - P_2)$ shear mode failure line exists for each particular crack length and that in the plot of f^3l^2 vs. P_2 the $(P_1 - P_2)$ shear mode locus cannot be a straight line butt must be a curve of decreasing slope, as indicated in Fig. 2. This provides one method of assessing whether fracture results are affected by bulging (P_2) effects, additional to observation of the fracture path.

Implications of Postulated Fracture Relationship

(a) Effects of variations in Charpy energy and yield strength

Consider that a pressure vessel stresses to a general stress level $(f_g)_1$ lower than that needed to produce failure.

As the temperature is lowered in the transition range the Charpy value of steel decreases sharply and the yield strength increases slightly, the net effect being to produce a reduction in the right hand side of equations (4). Hence if equations (4) are a sufficient statement of the critical conditions it might be thought that with the applied stress f_g held constant, a reduction

of temperature in this range could lead to a just sub-critical crack becoming critical.

However, a body of experimental evidence suggests that a further requirement must be met. It would appear that some degree of yielding or re-yielding immediately before fracture is essential, so that the conditions of equations (4) are not sufficient. The possibility of re-yield can be considered in terms of the requirements for extending the size (S) of the plastic zone at the end of a crack. Several authors (e.g. Dugdale(1), McClintock(20), and Irwin(21)) have quoted functions for determining (S) and these are shown in Fig. 3, together with experimental results determined in previous U.K.A.E.A. work(11).

All these results give linear log (S/l) vs. log (f_g/f_y) plots, although there are small differences in slope. A good approximation to cover these results is given by an equation of the form:

$$\frac{S}{l} = \text{const.} \times \left(\frac{f_g}{f_y}\right)^2 \qquad \ldots\ (5)$$

On this basis any slight increase of the material yield stress f_y produced by lowering the temperature would increase the stress needed to produce re-yielding and the initiation of an unstable crack. This implies that a vessel that has safely been pressurised at a higher temperature will not fail when pressurised to the same level at a lower temperature, even if the Charpy energy is reduced by the change in temperature. Similar arguments apply to the effect of irradiation and prolonged exposure to temperature, where these effects also cause decrease in fracture toughness in association with some increase in yield strength.

There are, however, limitations to reliance on this argument. The fundamental difficulty is that it is not proven rigorously that some yield is a necessary immediate prelude to fracture. Indeed in the case of ideally brittle materials this would appear not to be the case. The approach can only be used with caution, and is limited at the present time to relatively small degrees of embrittlement. In addition it is necessary to be certain that the pattern and nature of loading will be identical on the subsequent occasions. A further and important practical limitation is that it is generally necessary to consider the possibility of progressive crack extension in service.

Fatigue and/or creep mechanisms can lead to the initiation and growth of cracks in service, eventually extending to a critical size. As the crack increases in length, fresh material is enveloped by the plastic zone at the crack tip and hence it is to be expected that instability, when it occurs, will then be governed entirely by equation (4). The crack growth mechanism, however, must to some extent modify the material properties at the crack tip so that the critical crack length may be slightly different from the critical length for the single-loading case. Further, if the operating conditions of a pressure vessel were such that embrittlement of the shell material could occur then it would seem likely that this could have the effect of increasing crack growth rate through loss of cyclic ductility at the crack tip and in certain circumstances reducing critical crack size through reduction in Charpy value. Thus, the concept that initial pressurisation can give protection

against failure under subsequent more brittle conditions cannot be used without careful and detailed appraisal of each case.

(b) Decrease in yield strength f_y

As temperature is increased in the fully ductile range, yield strength decreases and therefore for constant values of f_g and l an increase in plastic zone size may be expected, in accordance with equation (5). This being so, it is to be expected that equation (4) would become the governing equation and cracks which were sub-critical at low temperatures could become unstable at temperatures where the yield is sufficiently reduced, Charpy energy φ remaining essentially constant. Such an effect is important in relation to proof testing pressure vessels and makes it necessary to carry out such tests at operating temperature or to make an allowance for the effect of temperature on yield strength and Charpy energy.

(c) Change of material

The previous paragraphs have considered the effect of changes in service to a design already constructed. It is sometimes necessary to consider the results of change from one material to another, at the design stage. In present design codes, the applied stress f_g is related to the yield strength f_y by a constant "safety" factor. Thus equation (4a) becomes:

$$(K_1 f_y)^3 l^2 = f_y^d f_u^e (C + D\varphi)$$

and for the same dangerous defect length:

$$\frac{K_2 f_y^3}{f_y^d f_u^e} = C + D\varphi$$

$$\text{i.e.}\quad f_y^{3-d} f_u^{-e} = C' + D'\varphi \qquad \ldots\ (6)$$

This implies that to get the same degree of confidence (i.e. protection at the permitted design stress against a defect of the same length l) it is necessary to increase the specified Charpy energy requirement with increased yield strength of the steel.

(d) Crack propagation

Once a crack has become unstable, the extent of fast crack propagation is primarily determined by the amount of energy involved and its availability at the crack front, i.e. the unloading path of the relevant part of the structure. Again, these considerations must also affect the crack speed and hence the strain rate experienced by the material in the crack tip region. In materials such as steel where the yield strength increases with strain rate, equation (5) indicates that increasing crack speed will cause the size of the plastic zone and hence the rate of dissipation of energy as plastic work in the crack tip region to decrease. This further upsets the balance between energy available and energy being dissipated and hence tends to cause an additional increase in crack speed. Thus it would appear that any trend in crack speed must to a certain extent be unstable. This suggests

that a crack initiated under shock conditions may be critical and capable of continued fast propagation at lengths less than those relevant to the static-loading case. Once such conditions have been established, it seems unlikely that the running crack can be arrested under conditions approximating to those of constant stress. The idea that a fast propagating crack, which has been triggered off by some transient and exceptional circumstances, will arrest at a certain temperature (C.A.T.) is undoubtedly a valid one when applied to structures which have a behaviour close to the constant-strain type, e.g. mechanically loaded structures and the corresponding Robertson test apparatus. It is equally certain and conclusively demonstrated in the pneumatically-pressurised vessel tests previously reported(11) that a running crack greater in length than the static critical length cannot be arrested by increase of temperature, in the constant-stress case of a large pressure vessel containing a compressible fluid. The arrest by increase of temperature of a sub-critical crack initiated by shock loading in a similar structure would necessitate a reducing strain rate effect on change of fracture type. Whilst this point has not yet been established, it is suggested that the widely used "transition temperature" approach is only of value in reducing the risk of the production of a critical crack by some transient and exceptional circumstance. The size of the plastic zone associated with a running crack determines whether the type of fracture surface is 45^{o} (shear) or 90^{o} (cleavage), the former occurring when the plastic zone size is greater than the plate thickness and the latter when it is less. Hence energy considerations also affect the fracture appearance and what appear to be completely brittle and completely ductile fractures can exist side by side in steel at the same temperature. Figures (4a) and (4b) show an example of this which occurred in the tests of reference 11. This in fact illustrates the lack of precision of these two terms "brittle" and "ductile" when applied in the context of fast fracture and the danger of the assumption that a particular type of fracture appearance in a service or test failure has any direct relation to the temperature at which failure occurred, or indeed any importance per se. Considerable confusion has arisen in previous treatments which have emphasised a transition in fracture appearance whereas the important concept from the viewpoint of safety is that of failure stress.

Periodic Proof Testing

The previous arguments and the experimental work previously reported (2, 11) show that the critical crack length/stress relation $f_g^3 l^2 = \text{const.}$ controls the onset of fast fracture in vessels of given material properties whilst for a vessel with varying material properties it is likely that the conditions for growth of a plastic zone (equation (5)) control onset of fast fracture.

It is possible to demonstrate by a suitable pressure test that no defect beyond a certain size exists in a practical pressure vessel. The critical size shown not to exist will be determined by the test pressure and temperature of the first pressure test, and it must be remembered that there may be cracks approaching the critical size under these conditions.

Given the necessary conditions a crack in a pressure vessel will grow under the influence of pressure cycles, and possibly creep. Thus Frost(14) says that if the parameter $f_g^3 l$ exceeds a certain value, then the crack will

grow. Further, relations of the form (2, 15):

$$l = l_o F(\text{stress or strain } N) \qquad \ldots. (7)$$

where l_o = original crack length

l = crack length after N cycles

F is a function of the bracketed terms

have been experimentally derived for the growth of cracks.

Provided that the pressure and temperature conditions of operation are less severe than those of the pressure test any near critical-crack at the test pressure will be considerably less than the critical size at the operating pressure. However, over a period of time such a crack may grow and eventually attain the critical size as governed by the operating pressure, leading to failure of the vessel under normal operating conditions. To prevent this, it is proposed to carry out a repeat over-pressurisation so that if a dangerous crack exists failure will occur under chosen conditions and at a chosen time when full safety precautions can be taken.

The time interval between such over-pressure tests will not be discussed and here, for the sake of simplicity, it will be assumed that the material properties do not change appreciably with time. The effect of varying material properties is discussed in more detail by Irvine et al.(2). Crack instability is then controlled by $f_g^3 l^2 = \text{const.}$, and crack growth by the empirical equation of the form $l_N = l_o F(N,e)$, where l_o = initial crack length and l_N is the crack length after N pressure cycles, each producing a strain range e. At the time of the pressure tests, it is assumed that a just sub-critical crack exists, of length l_o. Writing f_T for the gross area stress produced by the test pressure, the equation for instability is $f_T^3 l^2 = \text{const.}$

After an operating period covering N cycles, the crack grows to a length l_N where $l_N = l_o F(N,e)$ and if the length l_N is to be critical in conjunction with the gross area stress f_{op} produced by the operating pressure, then $f_{op}^3 l_N^2 = \text{const.}$

Hence

$$f_{op}^3 l_N^2 = f_T^3 l_o^2$$

$$\left(\frac{f_T}{f_{op}}\right)^{3/2} = \frac{l_N}{l_o} = F(N,e) \qquad \ldots. (8)$$

but f_T/f_{op} is equal to the test pressure ratio R, hence $R^{3/2} = F(N,e)$. Consequently if the crack growth equation is known the test pressure can be chosen to cover a certain operating period, and moreover it is not necessary to determine the actual length of any crack which may exist in the vessel.

The experimental programme discussed in the following section has been formulated from the foregoing theoretical considerations.

Experimental

In order to investigate the features discussed above an experimental study was made of the behaviour of steel cylinders containing simulated longitudinal faults which were in depth equal to the full wall thickness, in which a relationship was sought between initial fault length, temperature, stress at failure and material properties.

The full details of the experiments are reported elsewhere, (11,16) only the results being summarised here to provide a basis for discussion.

For the bulk of the work, cylindrical vessels 5 ft dia. x 14 ft long x 1 in. wall thickness were used. In addition a limited number of tests were conducted on vessels of 3 ft and 9 ft 6 in. diameter, again of 1 in. wall thickness and 14 ft length, to investigate the influence of diameter:wall thickness ratio.

The choice of material used in the basic investigation was influence by the following considerations. The pressurising medium was to be water which together with the simple heating and pressurising equipment used limited the test temperature to the range 0-100°C. This range should encompass both the brittle and ductile failure modes of the material selected which in all other respects should be comparable to a typical boiler-quality steel. These objectives were achieved by making two special casts of steel of rather elevated carbon content and reduced C:Mn ratio which were normalised after rolling at a relatively high temperature of 980°C.

Once an understanding of the main features of fault behaviour had been obtained the 5 ft vessel tests were extended to include several typical pressure vessel steels which were incorporated into the vessels in the form of large butt-welded panels, usually 8 ft x 4 ft in size.

Material Properties

(a) 0.36% C steel

This, the basic steel of the programme, was of analysis given in Table I(b). Mechanical properties of the steel were determined on plate off-cuts, stress relieved to the same cycle as the test vessels. These results were used as a guide in fixing the test conditions for vessels containing particular plates. In addition further tests were made on cut-outs from the actual vessels after pressurising to failure, care being taken to avoid material which had been plastically strained during the test.

The tensile strength of the material generally lay in the range 29-33 tons/in^2 with a yield strength of 14-17 tons/in^2. Elongations of 30-40% and reduction of area of about 50% were obtained, showing the material to be comparable to a nominal boiler-quality mild steel but of slightly increased strength and reduced ductility.

The Charpy V-notch tests showed the transition curve to be much less steep than that normally found, being in fact almost linear from fully brittle fracture at 0°C to fully ductile fracture at about 110-120°C. The energy

absorption in the fully ductile condition was in the range 40-70 ft lb, lying around 60 ft lb for most of the plates.

Isothermal crack arrest tests and Pellini drop weight tests were limited to the flat off-cut material from the plates used to make the earlier vessels. Both crack arrest (C.A.T.) and nil ductility temperatures (N.D.T.) generally lay in the 20-25°C range, just one giving a value of 35°C. No significant change in the C.A.T. occurred over the applied stress range of 8 to 16 tons/in^2. Comparison of flat-plate and vessel cut-out Charpy values showed the latter to be generally 10-20 degC higher in transition temperature, so the quoted C.A.T. and N.D.T. values could be lower than those obtaining in the vessels by this amount.

(b) Al-treated mild steel

Panels for insertion into the test vessels were formed from 1 in. thick plate rolled from a special cast of this steel which had been subjected to numerous and well-documented mechanical and crack arrest tests. The material analysis is given in Table I(b). The material had a tensile strength of about 28 tons/in^2, a yield strength of about 17-19 tons/in^2, with an elongation of 40% and reduction of area of about 70%.

(c) Low-alloy steel

Panels of this low-alloy (analysis in Table I(b)) steel were made from 1 in. plate which had been re-rolled from 3 in. Again tensile and Charpy specimens were taken from the panels after testing, the Charpy specimens being used to establish the very considerable range of scatter at the vessel test temperature. The material was of 40-42 tons/in^2 tensile strength, 31-34 tons/in^2 0.2% proof stress, with an elongation of 27-30% and reduction of area of 60%.

(d) Si-killed mild steel

One test was conducted on a formed panel of this steel (for analysis, see Table I(b)). Charpy specimens taken from the panel after testing were used to determine the energy absorption and fibrosity scatter at test temperature.

Test Vessels

The 5 ft and 3 ft dia. vessels were fabricated by cold-rolling two 84 in. wide plates to the appropriate diameter, welding longitudinally and then joining the two cylinders together and to torispherical heads of notch tough steel by circumferential welds. Each vessel was then stress relieved for two hours at 625°C and leak tested at 650 lb/in^2. A manhole was provided in one head to give interior access and other penetrations allowed filling, draining, heating, water circulation and air bleeding.

Faults of various lengths, representing full thickness cracks, were made longitudinally at the mid length of the vessel, i.e. the fault was normal to the central circumferential weld seam. Each vessel was tested with its longitudinal axis horizontal and the fault uppermost on the top centre line. The major portion of the fault length was flame cut; this length was extended

(beyond any heat affected areas) to within $\frac{1}{8}$ in. of its final length by sawing, and the final 1/16 in. at each end was cut with a thin hacksaw to give 0.008 in. wide notches.

Where tests were to be conducted on panels of other materials a large piece about 8 ft axially and 4 ft radially, usually containing the extended crack from a previous test, was cut from the portion of the cylinder opposite the longitudinal welds at the mid length position. Into this hole a panel of the test material, rolled to correct curvature, was butt welded; the whole vessel then being subject to stress relief, and the new fault being cut at the centre of the panel.

The faults were sealed to allow pressurisation by the application of thin aluminium patches covering the fault to the vessel interior and fixed in place by adhesive. The aluminium was then covered by a larger Neoprene patch secured by adhesive to prevent seeping of water under the aluminium at low pressures. Where a large amount of bulging was anticipated due to high pressures or large initial fault length, a narrow sheet-steel support was placed between the aluminium and the vessel wall to prevent the former being forced through the widening gap.

Test Method

The vessel temperature was controlled by passing hot water into the upper half of the vessel so that, over an area of 2 ft x 8 ft with the fault at its centre, the temperature variation rarely exceeded $\pm$ 1 degC. The variation around the circumference was small in the first few feet (less than 7 degC at 30 in. from the top centre line) but at the base of the vessel the temperature remained virtually at ambient in all the tests.

In the majority of tests, water was used as the pressurising medium. The vessel was placed in a concrete-lined pit, covered with sleepers to reduce the hazard from fragmentation, and heated to the test temperature. Because of ambiguity in failure conditions in high-temperature hydraulic tests, some tests were made using partially pneumatic pressurisation. In these cases gas pressure was applied to 15 ft long nylon and Neoprene bags placed within the vessel and having a volume of 10% or 20% that of the vessel. The remainder of the vessel was filled with water, retaining the same heating principle as in the hydraulic tests. The use of a gas bag avoided a gas sealing problem at the fault, and by holding the bag in the lower portion of the vessel by internal decking, no difficulties arose in heating the upper portion of the vessel. The gas volume was restricted to 10% or 20% to limit the explosive effect and to keep the exclusion limits for personnel within the site area. The risk of fragmentation prevented measurements being made of gap opening or of plastic zone size.

The vessels were placed on an open site and pressurisation was controlled from a bunker some 300 yards distant. Figures 5 and 6 show the before and after photographs of test V6T1. After attaining the test temperature, gas was admitted to the Neoprene bag (which was deflated during heating) displacing water through the outlet branch of the vessel until the desired gas volume was reached. The water bleed was closed and pressurisation to failure achieved by the discharge of 1980 lb/in^2 x 2000 ft^3 nitrogen cylinders

connected through 300 yards of copper piping to the vessel. The pressure at the vessel was read from the control bunker using a telescope sighted on a pressure gauge attached to the gas inlet branch on the vessel; the gauge could be read to an accuracy of about 10 lb/in^2.

The results obtained in all of these tests are summarised in Table II.

Test on Slotted Flat Plates

These tests were carried out on material similar to that of the vessel tests of one inch thickness. The specimens were in general 8 ft x 4 ft, the short direction being in the direction of stressing (Fig. 1). The ends were connected by pins to thick plates attached to the loading heads of the 4000 ton testing machine. Central slits were prepared as in the vessel tests, and the test temperature was carefully controlled. The results are summarised in Table III.

Discussion

Vessel Tests

The earlier results have been analysed in detail in previous papers (2, 11). Failure occurred under a wide range of conditions with general stresses less than needed to give general yield, and temperature dependence was small. An important conclusion is that the results show three types of failure, the cleavage and $(P_1 - P_3)$ types obeying the relationship: $f_g^2 l^2 \propto \varphi$. At higher Charpy values failure was by the $(P_1 - P_2)$ mode, as indicated by the degree of bulging and by the direction of the fracture. As indicated in Fig. 7, the failure condition in the $(P_1 - P_2)$ mode is very dependent on geometry.

Thus either increasing crack length, or reducing vessel diameter (and so necessitating a higher pressure for the same value of f_g) will increase P_2 negatively and cause the $(P_1 - P_2)$ mode for these particular configurations to fall below the extrapolated linear relationship. For example, considering the results for 5 ft dia. vessels only, it will be seen that the 24 in. crack failure line is below the 12 in. crack line. Again, considering only tests with initial fault length constant at 12 in., the effect of reducing the vessel diameter from 5 ft to 3 ft is to lower the value of $f_g^2 l^2$ at fracture.

In a previous paragraph it was pointed out that it was unlikely that failure would occur at a given applied stress, even at a lower temperature, after safe behaviour had once been shown at the same stress, provided that the possible growth of cracks between these events could be ruled out. A further possibility in this consideration is that the prior stressing at high temperatures leaves behind a residual stress pattern that actually helps to prevent subsequent failure, provided that harmful Bauschinger effects are not introduced.

Such a "hot pre-stress" effect has been demonstrated by Brothers and Yukawa (17), who introduced compressive stresses in the tip of a 0.4 in. notch using 2 in. square test pieces at temperatures above the Charpy transition. When these test pieces were tested to destruction, at temperatures below the Charpy transition, failure did not occur until the notch stress slightly

exceeded the initial pre-stress value, and the failure stress was directly dependent on the initial pre-stress level. Test pieces not subjected to warm pre-stressing failed at low levels of stress. Srawley and Beacham (18) and Kihara and Masubuchi (19) have also noted this effect. The latter authors say ".... it can be concluded that the specimen loaded to a certain value at high temperature cannot be failed at a stress lower than this preloaded value". An effect of this nature was shown in the present vessel tests by tests numbers V4T1 and V4T3.

In the first of these tests a 6 in. crack was cut in a vessel and the vessel was pressurised at 62°C to give a gross area stress of 14.7 tons/in^2. The vessel was cooled down to 12°C and again pressurised to the same value as before without failing. A test on a similar vessel with the same crack length, V1T2, failed at a stress level of 12.3 tons/in^2 at a temperature of 12°C. The increased failure stress in the pre-stressed case is believed to result from the compressive residual P_1 stress occurring on depressurisation, because the material at the crack tip yielded on the initial pressurisation at 62°C. The initial pressurisation at the higher temperature and pressure would create a larger plastic zone, and therefore higher residual stresses than would occur if the vessel had been previously pressurised to just under the failure condition for the cold test.

There is a tempting conclusion to be drawn from this, namely that once a pressure vessel has reached operating pressure and temperature, failure at any lower temperature is not possible unless the operating pressure is exceeded, provided that no significant non-pressure-dependent loads are applied to the vessel. Unfortunately all the previous evidence is based on flat-plate testing except for one test on a vessel, and this vessel had only a short crack. Consequently the effect of pressure bending the material surrounding the crack has been omitted by the very nature of the tests.

In the present series of tests, two tests (Nos. V7T11 and V11T4) were made in which the crack length was increased to allow for this effect. On re-testing these vessels at lower temperatures, failure occurred at approximately the same pressure as would have caused failure in a virgin vessel, i.e. no beneficial effect from the hot pre-stress occurred. It is suggested that this is because, as outlined in Appendix II, the bending action which occurs with the bulging around a long crack introduces tensile stresses at the crack tip on unloading, which counteract the compressive stresses introduced by the hot-pre-stress. Thus it may tentatively be concluded that a hot pre-stress effect will only occur in a vessel where factors inhibiting the effect of bending exist, i.e. a thick-walled large-diameter (and hence low pressure) vessel.

Flat-Plate Tests

The flat-plate experiments (Table III) appear to give conflicting results when compared with the results of the vessel tests under similar conditions (Table II), in so far as flat-plate tests give lower failure stresses at low temperatures, and higher failure stresses at high temperatures, even ignoring those tests in which instability was masked by repeated arrests. In an earlier paragraph it was suggested that this was because of the manner in which the applied stress load was distributed across the test.

To test this hypothesis, a considerable number of strain gauges were mounted on one plate, and readings taken at discrete load steps. The location of the strain gauges is shown in Fig. 8. The test plate was Si-killed steel 1 in. thick x 7 ft wide x 48 in. long, containing a 12 in. slit, the ends of the slit being 0.008 in. saw cuts. The total load applied to the specimen was increased in four stages from zero to 956 tons. Strain gauge readings were taken for each of these applied loads. The applied load was reduced to zero after each load application, so that any reverse yielding at the crack tip could be observed. The stresses derived from these strain gauge readings are listed in Tables IV and V. On completion of the test and after dismantling the loading plates, the vertical diameters on the $1\frac{7}{8}$ in. dia. holes in the cheek plates were measured. These are the holes through which pins are inserted, to pass through mating holes at the top and bottom of the specimen, and thus apply load to the specimen.

The vertical stress distribution along the top edge of the composite plate immediately under the loading pins is plotted for each value of applied load in Fig. 9. Fig. 10 shows the vertical stress distribution along the top edge of the Si-killed mild steel test length, and Fig. 11 shows a "contour map" of the vertical stress distribution over a quadrant of the composite specimen at the maximum applied load.

From Fig. 10 it will be seen that when the local stress is compared with the mean stress there is a very pronounced decrease in the vertical stress applied to the specimen immediately above the slit. Thus at 956 tons applied load, the vertical stress acting on the edges of the specimen increases from 5 tons/in^2 at the centre of the plate to 10 tons/in^2 at the edge of the plate. However, considering the vertical stress variation along the vertical centre line, the vertical stress at the slit is zero, and must increase to the applied stress at the load pins. A variation in vertical stress as shown by Fig. 10 would therefore be expected.

However, a considerably different loading pattern is shown by Fig. 9. This shows the variation of vertical stress in the composite specimen along a horizontal line approximately 5 in., below the loading pins. This distance should be sufficient for St. Venants' principle to apply. Thus at the lower applied loads (304 and 556 tons) the stress in the centre of the plate shows a marked increase over the general stress level, and only at the higher loads does a stress depression in the centre of the plate occur. This initial stress-peaking at low loads in the centre of the plate was most unexpected. However, the measurement on the holes in the cheek plates, through which loading pins were passed, showed that the vertical diameter of the holes at the outer edge of the plate had been elongated. In fact, there was a difference of approximately 0.010 in. in the vertical diameter of the outer holes compared with the holes in the centre of the plate. Obviously yielding of the outer holes had occurred, and most of this probably occurred on the very first test of this type, which had almost the highest value of applied load in the whole series. Consequently, when a specimen was attached to these yielded cheek plates in the subsequent tests, all the load is initially applied at the centre of the plate, because there is an initial clearance of 0.010 in. between the outer pins and the cheek plate holes. Only when this clearance has been taken up is the load applied towards the outer edges of the specimen.

However, in spite of these initial conditions, it will be seen from Fig. 9 that at an applied load of 956 tons the vertical stress at the edge of the specimen is 28% higher than at the centre of the specimen. It will also be seen that this difference increases with increasing load, and since even at 956 tons this specimen was well below fracture (a similar specimen tested at -25°C failed at an applied load of 1172 tons), then at the fracture load the stress differential from centre to edge of beam would be even greater. Thus, extrapolation of Fig. 12 to 1172 tons gives the differential to be 39%, and the fracture load would, of course, be greater than 1172 tons because the strain-gauged specimen was tested at 17°C.

The variation of the vertical applied stress at the centre and edge of the plate, as given by gauges 23, 4 and 22 respectively, is shown in Fig. 12.

From Fig. 12 it can be inferred that, at a total applied load of 670 tons, the vertical stress in the centre of the specimen is equal to the vertical stress at the edge of the specimen, so that, and for this load only, a uniformly distributed stress is applied to the specimen. Below this load the centrally applied stress is greater than the stress applied towards the edges of the specimen, and for loads greater than 670 tons the reverse holds true.

Thus the following conclusions can be stated for an 84 in. wide specimen containing a 12 in. slit and tested in this apparatus (subsequent to the yielding of the cheek plates in the first test). If fracture occurs:

(a) At an applied load of 670 tons, then a uniformly distributed stress is applied to the specimen. Consequently we have a valid test which can be compared with vessel tests.

(b) At an applied load of less than 670 tons, then the applied stress is concentrated over the slit, and is consequently greater than the mean applied stress. Hence in comparison with vessel tests we should find that the flat plate fractures at a lower mean applied stress than does a corresponding vessel.

(c) At an applied load greater than 670 tons, the reverse of (b) holds and a flat plate should fracture at a higher mean applied stress than does a corresponding vessel.

Figure 13 shows the hoop stress at failure plotted against temperature, previously reported (11) for 5 ft dia. x 1 in. thick, 0.36% C steel vessels containing 12 in. longitudinal slits. Plotted on this figure are the results from the only two 12 in. slit, pinned specimen tests with the 0.36% C steel, these results being marked A and B. The applied load at A is 548 tons, and at B 1142 tons.

It will be seen that these results are in accord with the arguments of (b) and (c) above, i.e. for point A the fracture load is less than 670 tons and the mean applied stress is less than for the corresponding vessel test, whilst at point B the fracture load is greater than 670 tons and fracture occurs at a mean applied stress greater than for the corresponding vessel test.

If the vessel failure curve is extrapolated, and joining points A and B, an intersection occurs at point C. This corresponds to a mean applied stress of 7.4 tons/in^2, and at this stress and this stress only, the vessel and plate tests correspond. Now a mean applied stress of 7.4 tons/in^2 requires in the 4000 ton machine a total applied load of (7.4 x 84 x 1 + a dead weight load of 52 tons). This is 674 tons, which is in agreement with the postulated total applied load of 670 tons, for vessel and plate comparity.

It will also be noted from Fig. 12 that as the applied load increases then the vertical stress at the edge of the plate and on the horizontal axis of the crack increases at a greater rate than either the central applied load or the applied load at the edge of the specimen. Thus at 1172 tons this stress would be beyond yield (13.8 tons/in^2) and it would not be unexpected if fracture initiated at some small defect at the edge of the specimen in the vicinity of the crack axis, instead of at the slit extremities. This would appear to have occurred in test P8 (see Fig. 14).

The extent of the area at the crack tips which undergoes reverse yield on unloading is surprising. Thus on unloading from 808 tons/in^2, reverse yield occurs over a length of up to 3 in. along the horizontal axis and measured from the crack tip.

Thus flat-plate tests give the same fracture results for cleavage propagation as 5 ft dia. vessel tests, provided that a uniformly distributed stress is applied to the plate. Such factors must be borne in mind in the interpretation of all flat-plate tests, and attempts are being made to redesign an apparatus to overcome the difficulties. It must be emphasised that these differences between the flat-plate and vessel tests do not arise from bulging effects, which do not arise until conditions of higher fracture toughness, when the $(P_1 - P_2)$ mode may occur in a vessel.

Practical Implications of the Results

The results of the series of vessel tests show that catastrophic failure at general stresses lower than those needed to cause general yield can occur over a wide range of temperatures and geometries, in vessels pressurised with a compressible fluid. The detailed examination of the associated flat-plate tests has shown that these low failure stresses over a wide range of conditions are not the result of bulging effects nor of the cylindrical geometry, as has previously been stated by others in the discussion of these results.

On the basis of this analysis, geometrical effects arising from bulging are only of significance when fracture occurs in a vessel as a result of $(P_1 - P_2)$ shear, a feature which can often be determined by direct observations of the nature of the crack. It is thus believed that the results reported are reasonably representative of the failure stress/defect size relationships to be expected over similar temperature ranges even in larger pressure vessels made from similar materials up to quite large levels of material toughness. From a 5 ft dia. x 1 in. thick vessel in mild steel, with a 12 in. crack, bulging effects would only appear to be important where the material shows more than at least 60 ft lb Charpy V-notch energy at the pressurisation temperature. The experiments with different pressurising media show that, whilst the initial failure stress is unaffected, the

possibility of subsequent arrest of a crack propagating from a critical defect depends on whether the structure behaves as in a constant-stress or constant-strain situation. The pressure vessel containing a compressible fluid approaches the constant-stress case, and will not permit the arrest of such a propagating crack. In such cases the interpretation of failure behaviour from fracture appearances can also be misleading.

These considerations suggest that the only method of guaranteeing pressure vessel safety is by knowledge of the failure instability stresses for corresponding defect sizes, and by knowledge of how such defects can grow. The only virtue of the "transition temperature" approach frequently used in pressure vessel safety arguments is to help to specify conditions under which a critical defect could not arise under transient and exceptional circumstances.

The results have shown that a relationship of the type:

$$f_g^3 l^2 = f_y^d f_u^e (C + D\phi) \qquad \left[\text{eqn (4)}\right]$$

is one condition which must be satisfied for unstable failure. It is believed that it also is essential with normal metals for yield to immediately precede fracture. The conditions for obtaining local yield are those for the extension of the plastic zone, the size of which has been shown to be governed by -

$$\frac{S}{l} = \text{const.} \times \frac{f_g^2}{f_y} \qquad \left[\text{eqn (5)}\right]$$

Under conditions of first loading, and other conditions when the failure path involves fairly extensive plastic flow at the crack tip, then the first requirement is the controlling one, and the experimental values can be used.

Under other conditions, equation (4) can be satisfied without failure occurring, because of the inability to produce re-yielding. This latter case is important in relation to the safety of pressure vessels operating at elevated temperatures, since the hot pre-stressing action of the previous on-power period will provide a substantial margin of protection against brittle fracture during a subsequent shut-down, particularly where bulging effects can be ruled out. Indeed the only way in which a brittle fracture could be initiated during such a shut-down in a thick-walled large-diameter vessel would be by the application of a loading which had a significantly different distribution from the normal pressure loading, had not been applied before and was of a sufficient magnitude to cause fast propagation of an otherwise sub-critical defect. In the case of a pressure vessel subject to the effects of neutron irradiation these same mechanisms will operate during shut-down. However, the probable increase in growth rate for any existing cracks as well as the reduction in Charpy energy in the ductile condition makes it seem likely that the conditions for fast crack propagation during on-power conditions could be reached in a shorter time than in the absence of irradiation, so that the effect of irradiation must be considered in such cases in detail.

Most pressure vessels are normally subjected to a proof pressure test after manufacture and before commissioning into service. The main objective in carrying out this test is usually to provide a demonstration that the vessel is able to withstand the principal service loading, i.e. pressure, and still have some margin of strength in reserve to accommodate other loadings. Loadings such as external moments on ducts are occasionally simulated during the test. There has been an increasing tendency recently to regard the proof test from a rather more exact viewpoint, i.e. as an inspection procedure which could reveal points of weakness. Given an adequate understanding of the modes of failure which are possible under the operating conditions, such a viewpoint appears quite plausible in the case of components of the vessel in which the operational loads are simulated during the test. Since cracks originating during manufacture may escape detection by conventional non-destructive techniques, the proof test may be regarded as providing assurance against the possibility of a vessel containing a defect approaching critical size going into service.

The analysis given in earlier paragraphs points out the possible existence of a failure path where, with the applied stress, defect size and material toughness constant, decrease in material yield strength (such as by increasing the vessel temperature) could lead to satisfying both equations (4) and (5) and so causing failure. For this reason it is important that an over-pressure test allows for the reduction in yield strength on increasing temperature to the operating level, possibly by doing such a test at maximum operating temperature. Such a high-temperature (340°C) test has recently been done on the pressure vessel for the Dragon reactor at Winfrith Heath.

Another point of practical importance relates to the specification of minimum Charpy energy levels for acceptable materials. Whilst the required levels indicated by the present vessel tests would be relatively low for practical levels of applied stress and defect size, the tests show that the level in the transverse direction is important. For a given degree of confidence it is necessary that the specified Charpy energy level increases sharply (possibly as the square) if full advantage is to be taken of materials of increased yield point.

The arguments above suggest that considerable protection against subsequent failure, and an estimate of the maximum defect size that can possibly exist, can be made from an initial over-pressure test satisfactorily carried out. The ability to guarantee failure safety then depends on the knowledge of the rate of growth of the postulated maximum possible defect. It is possible to transfer the risk of failure in service to specific occasions when prepared action can be taken by repeated over-pressurisation to controlled levels (usually of the order of safety valve settings) at chosen intervals in service. More detailed description of the philosophy of periodic proof testing is given in reference 2, the basic requirement being the possibility of making an estimate known to be pessimistic of the rate of growth of cracks approaching the critical size. Since such a philosophy can be a considerable help where the highest degree of confidence against failure is required, further work in the U.K.A.E.A. is aimed at studying crack growth in this range.

Acknowledgements

The authors gratefully acknowledge the contributions made by colleagues in the Reactor Materials Laboratory in discussion and to the experimental work referred to in this report.

References

1. Dugdale, D. S., Yielding of steel sheets containing slits. J. Mech. and Phys. of Solids, Vol. 8, 2 May 1960.

2. Irvine, W. H., Quirk, A. and Bevitt, E., Fast fracture of pressure vessels. J. Brit. Nucl. Energy Soc., January 1964.

3. Mills, B. D., Jnr., A mechanical spring analogy of a cracked sheet of metal. Welding Journal Res. Supplement, February 1962.

4. Winder, B., Vickers 4000 ton crack testing machine. Nuclear Eng., Vol. 7, 1962, pp. 61-63.

5. Sopher, R. P., Lowe, A. L., Martin, D. C. and Rieppel, P. J., Evaluation of weld joint flaws as initiating points of brittle fracture. Welding Journal, November 1959.

6. Lock, M. H., Gloria, R. and Sechler, E. E., Fatigue and penetration studies on pressurised cylinders. California Inst. Technology, Pasadena, Contract NAW 06431 Calcit 89.

7. Frisch, J., Comparison of semi-empirical solutions for crack propagation with experiments. Trans. Amer. Soc. Mech. Engrs., May 1958.

8. McEvily, A. J., Illg, W. and Hardrath, H. F., Static strength of aluminium alloy specimens. N.A.C.A. Tech Note 3816.

9. Ministry of Aviation, Unpublished report. Results quoted in A.R.C. Tech. Report CP.467, H.M.S.O., 1960.

10. Peters, R. W. and Kuhn, P., Bursting strength of unstiffened pressure cylinders with slits. N.A.C.A. Tech. Note 3993, April 1957.

11. Bevitt, E., Cowan, A. and Stott, A. L., Failure tests on cylindrical steel vessels containing axial faults. J. Brit. Nucl. Energy Soc., January 1964.

12. Aungst, R. C. and Defferding, L. J., Crack propagation tests on Zircaloy-2 reactor pressure tubing. HW-80567.

13. Griffith, A. A. The phenomenon of rupture and flow in solids. Phys. Trans. Roy. Soc., Vol. 221, 1921, p.163.

14. Frost, N. E., Relation between the critical alternating propagation stress and crack length for mild steel. Proc. Inst. Mech. Engrs., Vol. 173, No.35, 1959.

15. Frost, N. E. and Dugdale, D. S. The propagation of fatigue cracks in sheet specimens. J. Mech. and Phys. of Solids, Vol. 6, 1958, p.92.

16. Vaughan, H., Stott, A. L. and Cowan, A., To be published.

17. Brothers and Yukawa. Effect of warm prestressing on notch fracture strength. ASME Jnl. of Basic Eng., March 1963.

18. Srawley and Beacham. Crack propagation tests on high-strength sheet material: Effect of warm prestressing. N.R.L. Report 5460, April 1960.

19. Kihara, H. and Masubuchi, K., Effect of residual stress on brittle fracture. Welding J. Res. Supplement, April 1959.

20. McClintock, F. A. Discussion of paper on fracture testing of high-strength materials. Materials Research and Standards, April 1961, p.277.

21. Irwin, G. R., Fracture testing of high-strength sheet materials under conditions appropriate for stress analysis. N.R.L. Report 5486, 1960.

Appendix I

Stresses Acting At a Crack Tip

In a Flat Plate (Fig. 15)

(a) Principal stress P_1 normal to the crack axis

This stress arises from the stress concentration effect of the notch and is constant through the thickness (Fig. 16).

(b) Principal stress P_3

Figure 17A shows a cross-section through the plate along the crack axis. Stress P_1 does not act on the material to the left of the notch front AB; consequently there is no Poisson requirement for this material to contract. However, stress P_1 acts on the material to the right of the notch front AB, and there is a Poisson requirement for this material to contract in the thickness direction. Thus, for material in the notch vicinity an incompatibility exists; the material to the left of the notch exerts a restraining force on the material to the right of the notch. This produces the tensile stress P_3 to the right of the notch and the compressive stress to the left of the notch (Fig. 17A). Now because the plate is unloaded on the surfaces, the thickness stress P_3 must fall to zero at the surfaces and will vary through the plate thickness as shown in Fig. 17B; stress P_3 will increase with increasing plate thickness.

(c) Principal stress P_2 parallel to the crack axis

There are two components involved in this stress:

(a) The uniform longitudinal stress tends to open the notch, producing

a cantilever action. This effect introduces a tensile stress P_{2A} parallel to the crack axis which will be at its maximum value at the base of the notch.

(b) Because of the gradient of P_1 in the direction normal to the crack axis the material in the notch base wishes to contract more along the crack axis (Poisson effect) than does the material immediately either side of the crack axis. This incompatability introduces a tensile stress P_{2B} along the crack axis (Fig. 18).

In a Pressure Vessel

For a longitudinal crack in a large cylindrical pressurised vessel, two additional factors to the flat-plate case are introduced in the crack tip stress system:

(a) A uniform pressure stress P_{2L} along the crack axis, where

$$P_{2L} = \frac{P_1 D}{4t}$$

(D = vessel diameter, t = plate thickness) arising from equilibrium conditions.

(b) The gas pressure acting on the material unsupported by the crack results in an encastre beam effect. Thus bending stresses P_{2M} act in the material at the crack tip in the P_2 direction. The stresses are compressive on the outer surface of the plate and tensile at the inner plate surface.

Summarising these stress conditions at a crack tip for a plate and pressurised vessel respectively:

(a) Plate

The stress P_1 is constant through the thickness.

The thickness stress P_3 is 0 at plate surfaces and increases to a tensile maximum at mid-thickness.

The stress P_2 comprises: P_{2A}, from cantilever action, which is a tensile stress uniform through the plate thickness; and P_{2B} from Poisson incompatibility.

(b) Pressure vessel

The plate stresses summarised above act at the tip of a longitudinal crack in a pressure vessel together with the following stresses acting along the crack axis:

$P_{2L} = \frac{PD}{4t}$, a uniform tensile pressure-dependent stress through the thickness.

P_{2M} bending stress, at a maximum negative value on the outer surface, and a maximum value on the inner surface.

A third compressive stress will also act in the radial direction, having its maximum value on the inner surfaces of the vessel and being equal to the gas pressure and therefore of negligible magnitude in "thin" vessels.

Appendix II

Effect of Bending Over the Crack Length on the Residual Stresses at the Crack Tip

Consider a section through the crack axis (Fig. 19), XX_1 representing the crack tip and the section to the left of XX_1 the crack. Then when internal pressure is applied there will be an encastre beam effect. If we now superimpose the various stresses acting in the longitudinal direction we have a net tensile stress P_{2L} acting through the thickness (Appendix I) and using XX_1 as the datum line P_{2L} is represented by line AA_1, i.e. $XA = P_{2L}$. The bending stress has now to be superimposed on this stress; the resultant stress is given by the line BB_1. If local bulging occurs over the crack length, yielding must have occurred, and with $X_1 f_y$ representing the value of the yield stress the area Cf_yB_1 cannot exist and must be replaced by an equal area below f_y, area CDE. The location of B may be either to the left or right of point X, i.e. a compressive or tensile stress may act a point X on the outer surface. As discussed earlier, if a compressive stress exists then $(P_1 - P_2)$ shear failure will occur, and if a tensile stress exists the $(P_1 - P_2)$ shear failure will occur. However, the position of point B does not affect the present argument.

Now unload the vessel, and remove the stresses in turn, with P_{2L} being removed first, and finally the elastic bending stress. Then after removal of P_{2L} (equal to length XA) the distribution is given by JHGF. Removal of the bending stress (given by ABB_1A_1) from JHGF gives the residual stress distribution KLMP after complete load removal.

Thus a large tensile stress of magnitude given by the ordinate from XX_1 to M, i.e. NM, exists in the centre of the plate, and moreover this stress has steep gradients. Thus the material at N, owing to the Poisson requirement, wishes to contract in the hoop direction because of stress NM, whereas the material immediately above this has no such requirement. Consequently this material will restrain the material at N causing a tensile stress to act at N in the hoop direction.

Thus because of the effect of bulging, a residual tensile stress has been caused in the hoop direction.

Table I(a)

Dia., in.	Crack length, in.	Hoop stress, lb/in^2	$\left(f^2 l\right)^{\frac{1}{2}}$	$\left(f^3 l^2\right)^{\frac{1}{3}}$
0.25	0.59	678	240	125
0.32	0.71	590	232	128
0.38	0.74	526	229	128
0.28	0.61	655	245	130
0.26	0.62	674	243	128
0.30	0.61	616	238	128

Table I(b)

Analysis of test materials, %

	C	Mn	Si	S	P	Ni	Cr	Mo	Cu	V
0.36% C	0.36	0.44-0.46	0.10-0.13	0.038-0.024	0.015-0.024	-	-	-	-	-
Al-grain-refined steel	0.13	1.14	0.12	0.003	0.015	-	-	-	-	-
Si-killed steel	0.16	1.22	0.20	0.03	0.014	-	-	-	-	-
Low-alloy steel	0.155	1.30	0.22	0.02	0.022	0.22	0.63	0.255	0.07	0.09

Table II

Summary of results from vessel tests

Material	Vessel and test no.	Plates	Initial fault length (in.)	Test temp. (°C)	Gross area stress at failure f_g (tons/in^2)	$f_g^3 l^2$ (l = fault half length, in.) x 10^{-3}	Vessel cut-out data: Tensile data specimens // to rolling direction, i.e. in direction of vessel hoop stress: U.T.S. (ton/in^2)	Y.P. (ton/in^2)	E(%)	R of A (%)	Charpy V-notch values at test temp.: Energy (ft lb) Range	Energy Mean	Fibrosity (%) Range	Fibrosity Mean	Stress-relieved off-cut data: Robertson isothermal C.A.T. (°C). Stress (ton/in^2) in brackets	Nil ductility temp. (°C)	Type of failure	Remarks
0.36% C	V1T2	A	6	12	12.3	17	29.6	15.9	38	50	8-11	9.2	15-20	16.1	>19<23 (8)	15	P_1	Hydraulic test.
		B					29.7	14.9	38	51					<10 (4)			
							31.3	17.9	35	50	5-9	7.7	3-8	5.2	>15<19 (8)			
							3.2	16.8	34	49					>20<30(14)			
															<30(16)			
0.36% C	V5XT1	F	6	45	14.4	27	32.0	15.0	35	50		18		25			P_1	10% pneumatic test
		M					32.4	17.4	34	49								
							32.4	16.4	37	51		21		32	>20<25 (8)	20		
							31.1	15.0	37	50								
0.36% C	V4T1	I	6	62	14.7	29	29.2	14.4	39	56		42		55	>20<25 (8)	20	Uncertain because of small extension, probably P_1	Hydraulic test
		R					29.2	13.8	38	55								
							33.2	16.6	35	48		21		33				
							33.2	16.4	32	46								
0.36% C	V4T2	I & R R	7.5	50	14.7 (unfailed)				As above			35 17		40 28				Hydraulic test Demonstration of hot pre-stress effect
0.36% C	V4T3	I & R R	7.5	12	14.7 (unfailed)				As above			8 6		10 10				Hydraulic test
0.36% C	V2T1	C	12	29	8.4	21	37.0	15.2	35	52		14*		18*				
		Q					31.4	15.6	35	51								
							31.2	14.6	35	52		14*		18*		25		
							31.2	14.6	35	51								
0.36% C	V8T1	H	12	7	4.0	23	-	-	-	-							P_1	Hydraulic test. Failed at half the predicted value. Subsequent investigation showed that in the fault preparation residual tensile stresses had arisen at the fault tip.
0.36% C	V8T2	H	12	13	8.0	18						16*		11*			P_1	Hydraulic test. Repeat of V8T1 but avoiding residual stress at fault tip. F_g as predicted.
0.36% C	V4T4	I R	12	51	9.4	30			As V4T1		15-23 23-38	18.8 29.3	30-30 30-45	30 39.4			P_1	Hydraulic test

*Indicate that figures are taken from transition curve

(Continued)

Table II (Continued)

Material	Vessel and test no.	Plates	Initial fault length (in.)	Test temp. (°C)	Gross area stress at failure f_g (tons/in²)	$f_g^3 l^2$ (l = fault half length, in.) x 10^{-3}	Vessel cut-out data: Tensile data specimens // to rolling direction, i.e. in direction of vessel hoop stress — U.T.S. (ton/in²)	Y.P. (ton/in²)	E(%)	R of A (%)	Vessel cut-out data: Charpy V-notch values at test temp. — Energy (ft lb) Range	Energy (ft lb) Mean	Fibrosity (%) Range	Fibrosity (%) Mean	Stress-relieved off-cut data: Robertson isothermal C.A.T. (°C). Stress (ton/in²) in brackets	Stress-relieved off-cut data: Nil ductility temp. (°C)	Type of failure	Remarks
0.36% C	V6T1	L	12	77	11.5	55	31.0	14.8	30	48		34		55			P_1 - P_3	20% pneumatic test
		N					34.6	14.4	33	48		35		50				
0.36% C	V5T1	F M	12	84	11.9	61			As V5XT1		32-45 41-50	37.7 45.7	40-60 75-80	46.6 77.7			P_1 - P_2	Hydraulic test
0.36% C	V7T11		12	a) 80	9.9 (unfailed)												P_1	Hydraulic test. Attempt to demonstrate 'hot pre-stress' effect with longer fault See text for discussion
				b) 10	7.1	13					5-9	7.2	5-10	6.5				
0.36% C	V11T6		12 at 45° to plate surface	80	11.5	55											P_1 - P_3	Hydraulic test to examine effect of orientation of initial defect on initiation of failure.
0.36% C	V7T1	O U	24.75	1	4.3	12					3-10	6.5*	2-12	7*			P_1	Hydraulic test
0.36% C	V3T1	E V	24	62	5.7	27	35.6 35.9	16.0 16.0	29 31	41 42	19-27	22.1	35-50	40.5	>30<35 (8)	35	P_1	Hydraulic test
							32.0 32.7	15.2 17.2	35 35	51 50	19-26	22.2	35-35	35				
0.36% C	V3XT1	E V	24	88	6.8	45	As above				31-47 41-45	37.7 42.5	40-55 80-90	46.1 85	As above		P_1 - P_2	20% pneumatic test
0.36% C	V13T1 3' 0" dia.	P	12	10	6.2	9					5-7	6.5	3-5	3.6			P_1	Hydraulic test
0.36% C	V12T1 3' dia.	W	12	79	10.45	41					35-46	40	70-80	75			P_1 - P_2	Hydraulic test
0.36% C	V12T3 3' dia.		12	50	7.8	17					13-15	13.7					P_1	Hydraulic test
0.36% C	V14T2 Panel 9' 6" dia.		12	17	9.0	26					4-6	5.2	3-5	4.1			P_1	Hydraulic test

*Indicates that figures are taken from transition curve

(Continued)

Table II (Continued)

Material	Vessel and test no.	Plates	Initial fault length (in.)	Test temp. (°C)	Gross area stress at failure f_g (tons/in²)	$f_g^3 l^2$ (l = fault half length, in.) x 10^{-3}	Vessel cut-out data: Tensile data specimens // to rolling direction, i.e. in direction of vessel hoop stress — U.T.S. (ton/in²)	Y.P. (ton/in²)	E(%)	R of A (%)	Vessel cut-out data: Charpy V-notch values at test temp. — Energy (ft lb) Range	Energy (ft lb) Mean	Fibrosity (%) Range	Fibrosity (%) Mean	Stress-relieved off-cut data: Robertson isothermal C.A.T. (°C). Stress (ton/in²) in brackets	Stress-relieved off-cut data: Nil ductility temp. (°C)	Type of failure	Remarks
0.36% C	V14T1 9' 6" dia.	Panel	12	80	12.1	63					23-27	25					P_1 - P_2 (probably)	Hydraulic test
Aluminium grained refined steel	V7T5		12	16	13.3	85	28.6	18.8	41	68	61-78	69	70-80	74.7			P_1 - P_3	Hydraulic test. Plate mounted transversely to present minimum Charpy to crack.
							28.6	19.5	40	68								
"	V9T1		12	18	14.2	103		-	-		94-118	108.9	70-85	79			P_1 - P_2	10% pneumatic test
"	V7T2		12	49	13.1	81	27.8	16.8	43	72	119-126	122.5*	100	100*	>-10°C <-5°C	-20	P_1 - P_2	Hydraulic test. Crack only extended 0.1". Probably rogue result. cf. V9T1 and V10T2.
"	V10T2		12	79	14.2	103					112-220	115	100	100*			P_1 - P_3	10% pneumatic test
"	V7T3		24	19	8.7	95		0.2%			102-115	108.5	72-73	72.5			P_1 - P_3	10% pneumatic test
Low alloy steel	V7T6		24	9	7.6	63	40.0	31.4 (0.2%)	29	60	27-68	36.2	35-100	49.2			P_1	Hydraulic test. R.O. of panel perp. to hoop stress. (Plate mounted transversely)
"	V7T10		24	56	9.2	112	42.2	33.6 (0.2%)	27	56	106-117	111.5	100	100			P_1 - P_2	Hydraulic test
							42.1	33.2	27	60								
"	V11T3		24	23	10.45	164					68-103	83	60-100	72			P_1 - P_2	Hydraulic test
"	V11T4		29	40	5.9	43					6-27	15.4	0-5	2.2			P_1	Hydraulic test. Attempt to find hot pre-stress effect on fault left after V11T3
Silicon killed steel	V7T4		12	39	12.7	75	28.6	13.8	40	60	50-68	58.6	55-80	63.9		-5	P_1 - P_2	

*Indicates that figures are taken from transition curve

Table III

Results of flat plate tests

Steel type	Specimen no.	Plate width (in.)	Crack length (in.)	Temperature (°C)	Nominal applied stress at fracture (tons/in²)
0.36% C	P.1	84	12	16	13.0
	P.2	84	24	18	$9.2 < f_g < 10.4$
	P.3	84	24	-20	6.2
	P.4	84	12	-22	5.9
	P.5	84	24	47	$8.1 < f_g < 8.6$
	P.6	60	27	17	8.1
Silicon-killed steel	P.7	84	36	-20	8.9
	P.8	84	24	-19	12.5
	P.9	84	24	-46	12.9
	P.10	84	12	-25	13.3
Aluminium-grain-refined steel	P.11	84	24	-30	No failure at 19.1
	P.12	84	36	-50	No failure at 21.9

Notes: All plates 1 in. thick

Nominal applied stress is load divided by (plate width x thickness).

Table IV

Horizontal and vertical stresses derived from Huggenberger extensometer readings

Total applied load (tons)	Gauge pairs. Stress readings are in tons/in² 1,26	2,25	3,24	4,23	5,21	6,20	7,19	8,18	22	12,13	11,14	10,15	9,16	17
152	1.17	0.94	1.52	2.26	1.24	1.45	1.02	1.25	0.64	13.95	3.93	3.05	2.64	0.75*/
	-0.82	0.28	0.46	0.47	-0.46	0.22	0.20	0.27		7.6	1.07	0.28	0.06	
0										0.53				
										1.1				
556	3.91	3.85	4.08	4.78	4.25	4.14	2.95	3.34	3.83		9.44	8.42	6.55	4.25
	-0.42	1.15	1.23	1.44	0.0	0.71	1.10	1.21		Y(25)	3.14	1.89	0.94	
808	6.55	6.90	6.50	6.62	7.30	6.63	4.94	4.50	7.65			12.15	10.78	8.72
	-0.13	1.75	1.84	2.20	0.60	0.82	1.59	1.88		Y	Y(23)	3.13	1.96	
956	8.9	7.64	7.85	7.76	8.97	7.82	5.80	5.11	10.00			Y(16.6)	Y(14.7)	11.80
	2.35	-1.11	2.46	2.86	0.89	0.97	1.95	2.17		Y	Y	5.09	2.92	

* Vertical stress

/ Horizontal stress

Y indicates stresses above yield
Calculated stress in brackets

Stress range on unloading			
556 tons to zero	-27		
	-13		
808 tons to zero	-53	-13	
	-20	-5	
956 tons to zero	-74	Off	
	-38	scale	

Vertical stress range
Horizontal stress range

Note: For calculation of these stresses the following assumptions were made:

E = 29×10^6 lb/in²
Poisson's ration = 0.3
Yield point = 13.8 tons/in² (not an assumption)

Table V

Horizontal and vertical stresses derived from resistance strain gauges (tons/in^2)

Total applied load (tons)	Strain gauge rosette no.											
	1		2		3		4		5		6	
	p_x	p_y	p_x	p_y	p_x	p_y	p_x	p_y	p_x	p_y	p_x	p_y
304	0.6		1.2		1.7		1.0		0.25		1.6	
		4.4		5.2		4.1		6.2		4.6		2.5
556	0.8		1.4		2.0		0.9		0.20		1.7	
		6.3		7.2		5.4		9.0		7.4		2.55
808	0.05		0.95		2.3		0.15		-0.85		1.55	
		9.2		8.2		5.7		11.4		6.15		2.5
956	0.4		1.1		1.5		-0.025		-1.25		0	
		10.3		8.75		6.1		12.3		6.15		2.1

p_x = horizontal stress

p_t = vertical stress

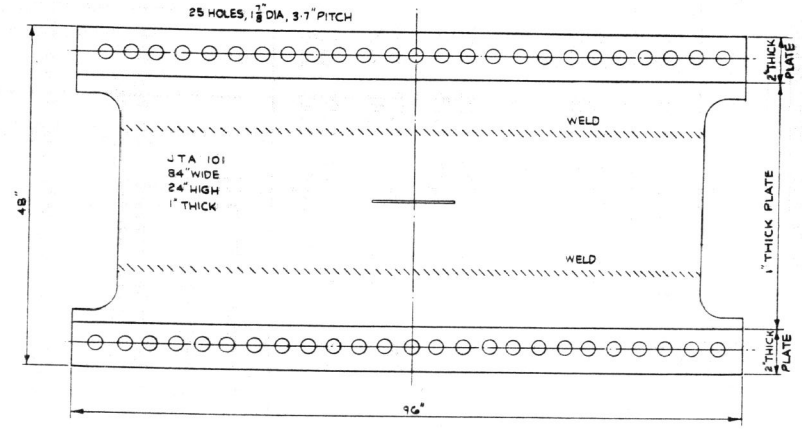

FIG.1. ESSENTIAL DIMENSIONS OF COMPOSITE SPECIMEN FOR SLOTTED FLAT PLATE TESTS

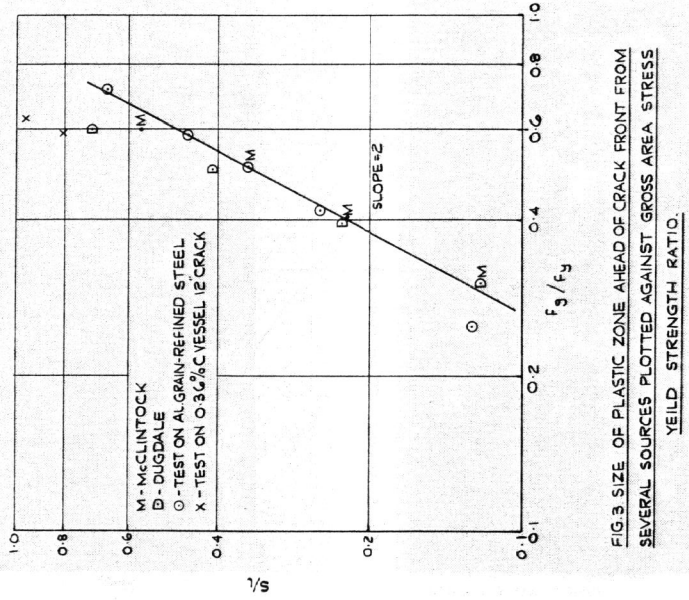

FIG.3. SIZE OF PLASTIC ZONE AHEAD OF CRACK FRONT FROM SEVERAL SOURCES PLOTTED AGAINST GROSS AREA STRESS YEILD STRENGTH RATIO.

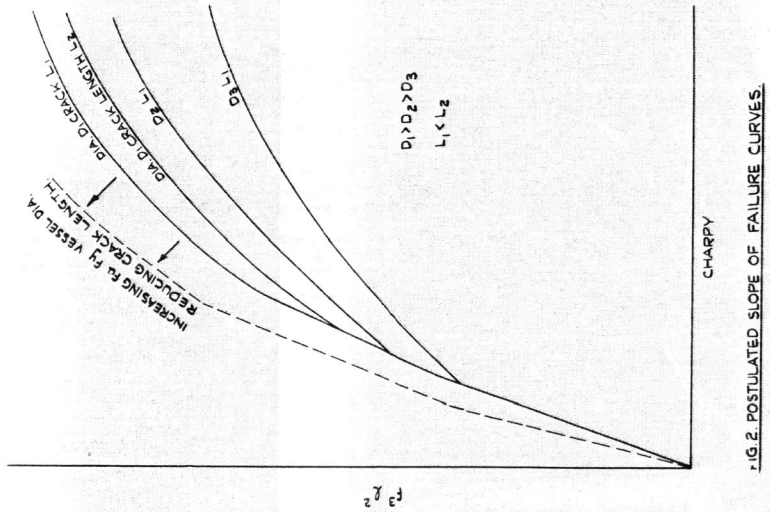

FIG.2. POSTULATED SLOPE OF FAILURE CURVES.

Fig. 5 Vessel V6T1 on open site prior to 20% pneumatic test

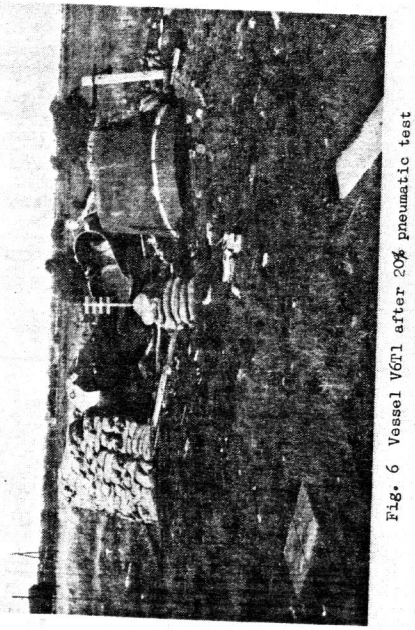

Fig. 6 Vessel V6T1 after 20% pneumatic test

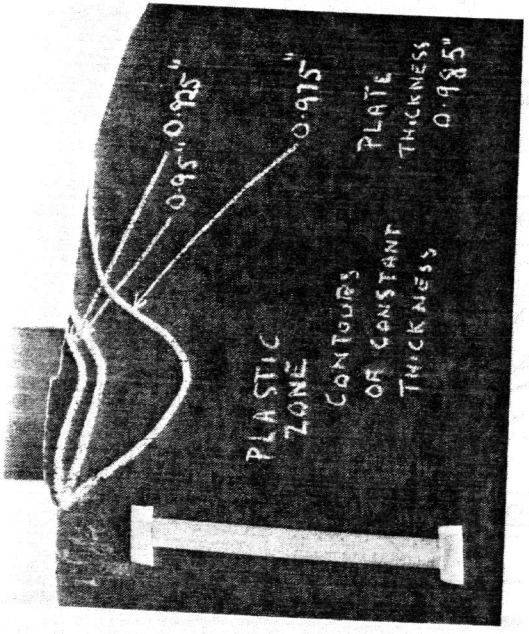

Fig. 4 (a) Reduction in thickness at fracture edge
(b) Change from 45° to 90° fracture with decrease in plastic zone size

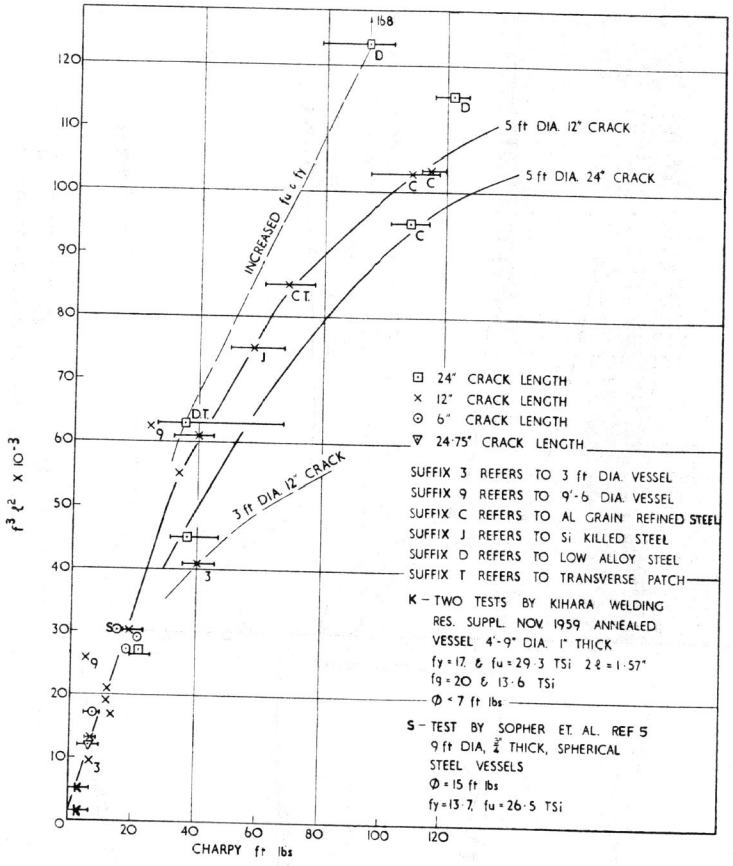

FIG. 7. CHARPY v $f^3 \ell^2$ FOR TEST VESSELS.

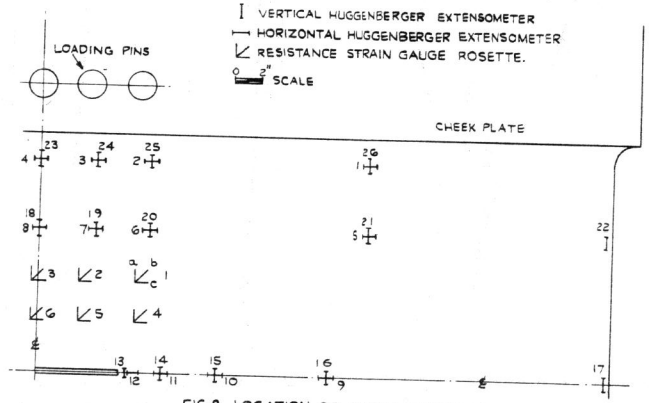

FIG.8. LOCATION OF STRAIN GAUGES.

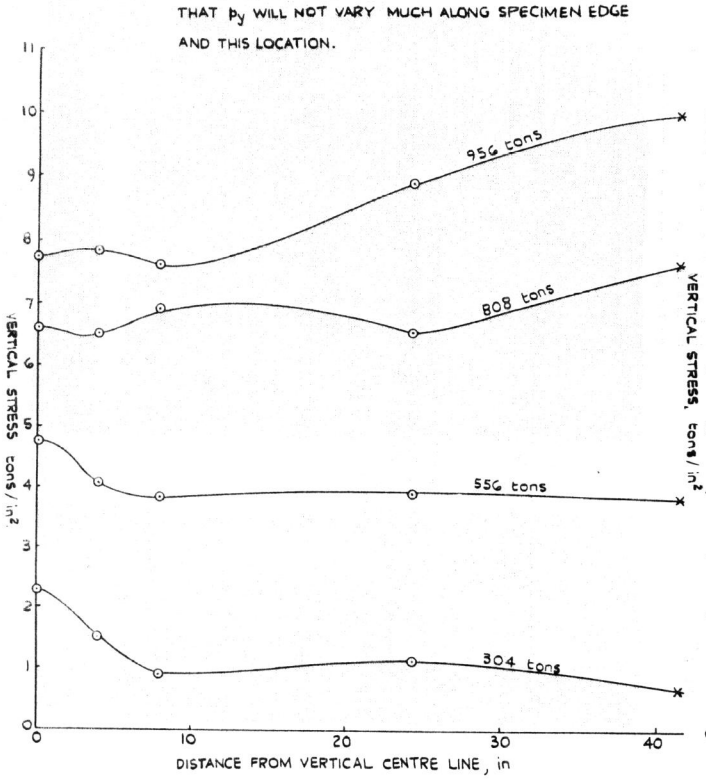

FIG.9. VERTICAL STRESS DISTRIBUTION ALONG TOP EDGE OF COMPOSITE SPECIMEN (i.e. ALONG HORIZONTAL LINE THROUGH GAUGES, 23/4, 24/3, 25/2 AND 26/1)

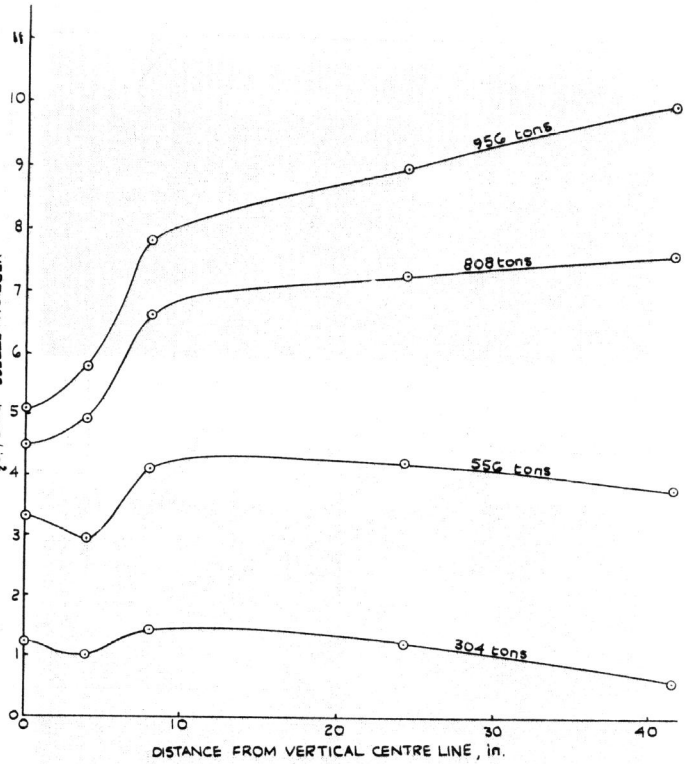

FIG.10. VERTICAL STRESS DISTRIBUTION ALONG TOP EDGE OF TEST SPECIMEN (i.e. ALONG HORIZONTAL LINE THROUGH GAUGES 18/8, 19/7, 20/6, 21/5 & 22)

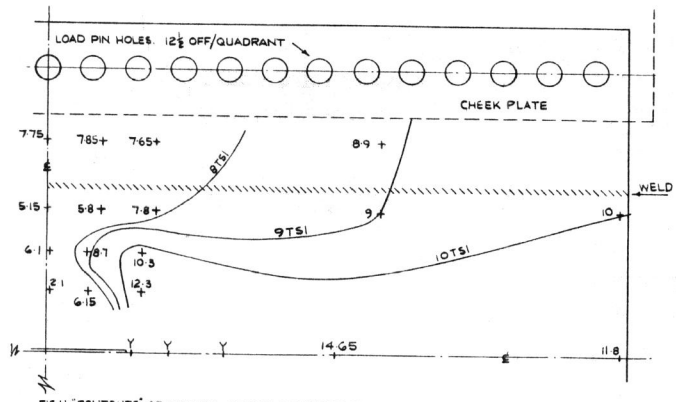

FIG.11. "CONTOURS" OF VERTICAL STRESS DISTRIBUTION IN QUADRANT OF COMPOSITE SPECIMEN AT MAXIMUM VALUE OF APPLIED LOAD (956 ton)

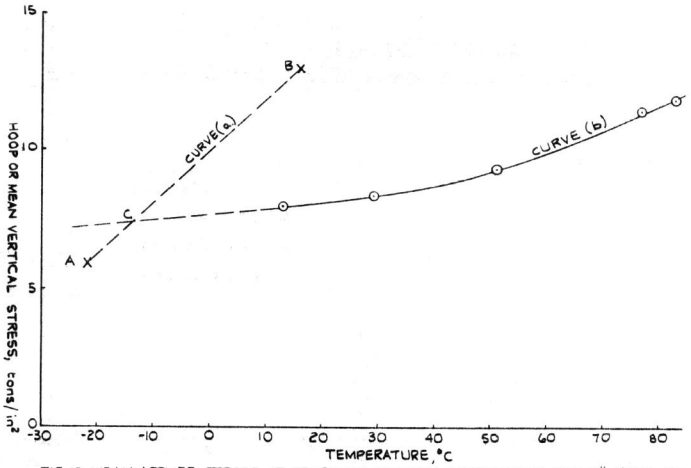

FIG.13. MEAN APPLIED STRESS AT FRACTURE AGAINST TEMPERATURE FOR 12" SLITS IN (a) 84" WIDE, ·36%C FLAT PLATE SPECIMENS, (b) 5Ft DIA, ·36%C STEEL VESSELS

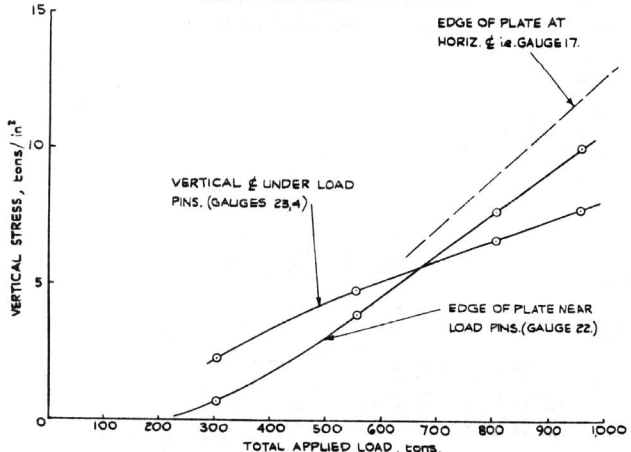

FIG 12. SHOWING HOW THE VERTICAL STRESS AT THREE LOCATIONS IN THE PLATE INCREASES WITH APPLIED LOAD.

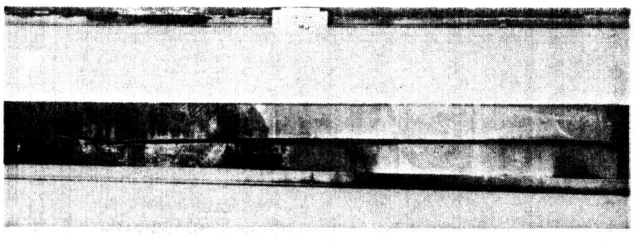

Fig.14 Initiation of crack at edge of slotted flat plate specimen

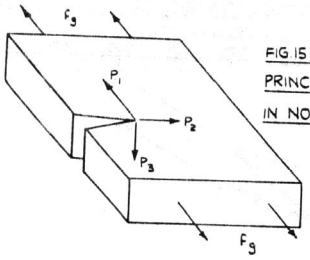

FIG.15 NOMENCLATURE OF PRINCIPAL STRESS SYSTEM IN NOTCHED PLATE.

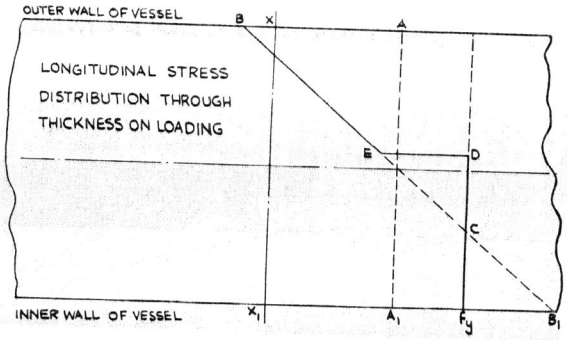

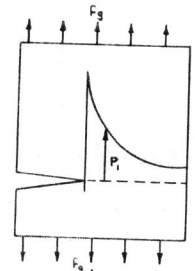

FIG.16. VARIATION OF P_1 ACROSS PLATE WIDTH.

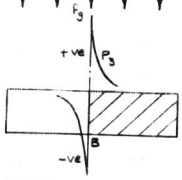

FIG.17 (A) VARIATION OF P_3 ACROSS PLATE WIDTH.

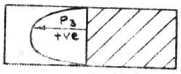

FIG.17(B) VARIATION OF P_3 THROUGH PLATE THICKNESS.

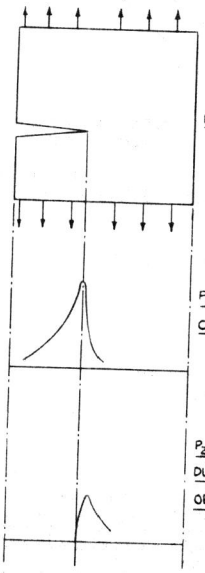

FIG.18 VARIATION OF WIDTH, P_2 STRESSES

P_{2A} STRESS DUE TO CANTILEVER ACTION.

P_{2B} STRESS DISTRIBUTION DUE TO INCOMPATABILITY OF WIDTH CONTRACTIONS.

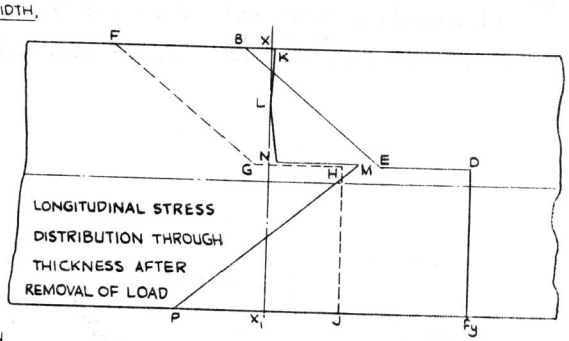

FIG.19 DEVELOPMENT OF RESIDUAL TENSILE STRESSES AT CRACK TIP DUE TO BULGING.